International Journal of Bifurcation and Chaos, Vol. 9, No. 7 (1999) 1321–1331

SYMMETRY, GENERIC BIFURCATIONS, AND MODE INTERACTION IN NONLINEAR RAILWAY DYNAMICS

CARSTEN NORDSTRØM JENSEN*
ES-Consult Ltd, Staktoften 20, DK-2950 Vedbæk, Denmark,

MARTIN GOLUBITSKY†
Department of Mathematics, University of Houston, TX 77204-3476, USA

HANS TRUE‡
The Technical University of Denmark, Department of Mathematical Modelling, Building 321, DK-2800 Lyngby, Denmark

Received June 29, 1998; Revised February 4, 1999

We investigate Cooperrider's complex bogie, a mathematical model of a railway bogie running on an ideal straight track. The speed of the bogie v is the control parameter. Taking symmetry into account, we find that the generic bifurcations from a symmetric periodic solution of the model are Hopf bifurcations for maps (or Neimark bifurcations), saddle-node bifurcations, and pitchfork bifurcations. The last ones are symmetry-breaking bifurcations. By variation of an additional parameter, bifurcations of higher degeneracy are possible. In particular, we consider mode interactions near a degenerate bifurcation. The bifurcation analysis and path-finding are done numerically.

1. Introduction

In this article we investigate some dynamical features of the Cooperrider bogie [Cooperrider, 1972]. A modern railway passenger car has a car body supported at each end by a carriage or *bogie* with a relatively short wheel base. See Fig. 1. The suspension systems are placed in the bogies and between the bogies and the car body. Since the guiding forces from the rails act on the wheelsets in the bogies, the bogies play an important role in the dynamics of the vehicle motion.

The mathematical model is presented at the end of this section. The model has been treated in several articles. In the survey article by True [1993] a bifurcation diagram shows the most important features of the system. However this diagram is incomplete and refined investigations by Jensen [1994] complete the bifurcation diagram. Jensen and True [1997] treat the appearance of quasiperiodic and chaotic motions in a small speed interval. Galvanetto *et al.* [1997] find an optimal wheel base by varying another parameter in the system.

In Sec. 2 we outline the mathematical theory related to our investigations of this model and we use the symmetry of the model to deduce the form that generic bifurcations from symmetric periodic solutions will have. In contrast to systems without symmetry, period-doubling bifurcations are not

*Author for correspondence.
E-mail: cnj@es-consult.dk
†E-mail: mg@uh.edu
‡E-mail: ht@imm.dtu.dk

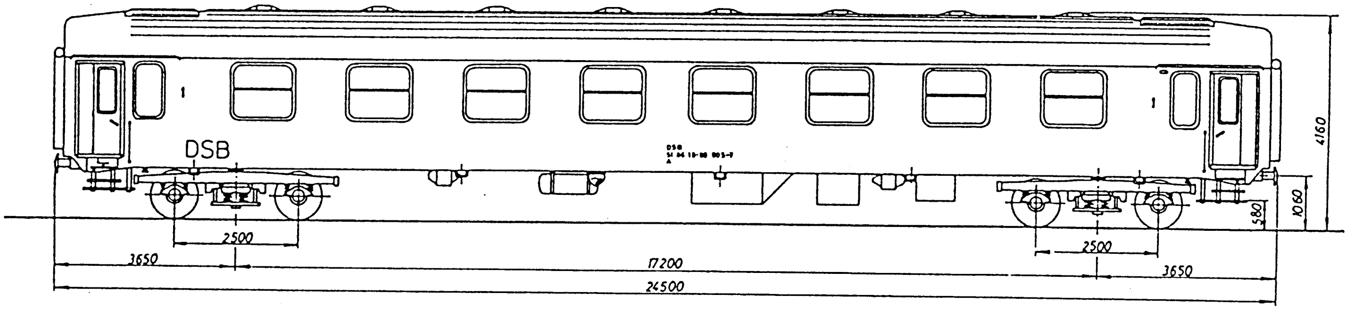

Fig. 1. Danish passenger coach on two bogies.

generic, but symmetry breaking pitchfork bifurcations are. This remark was noted previously by Swift and Wiesenfeld [1984] and by Fiedler [1988]. If two critical eigenvalues are close in the control parameter space, different types of secondary bifurcations may occur. This type of degeneracy is called *mode interaction.* In our model equations we find a mode interaction between a saddle-node and a pitchfork bifurcation. This mode interaction studied by Dangelmayr and Armbruster [1983], has been reported in [Golubitsky *et al.*, 1988], and explains a number of features in the bifurcation diagram of the Cooperrider model.

The results of our numerical investigations, showing various kinds of generic bifurcations as well as mode interactions, are presented in Sec. 3. The mathematical theory verifies the numerical results. The stringent mathematical theory suggested a generic interpretation of the numerical results and led to the discovery of the correct splitting and the correct sequence of the bifurcations of the periodic attractor. It also helped the authors to look for and find a solution that had not been found before due to its instability and/or small basin of attraction.

Section 4 contains the conclusions.

1.1. *Dynamical Model*

The Cooperrider model [Cooperrider, 1972] was developed as a model for a conventional passenger car bogie with two axles. We assume that all parts except the suspension elements are rigid and that the suspension elements all have linear characteristics. Furthermore, we assume that the vertical displacements are so small that the equations for the vertical and horizontal motions are uncoupled. We are only interested in the lateral motion.

The model of the conventional bogie is a multibody system. The bogie frame can rotate without friction in a bearing in the floor of the car body. It is supported on two wheelsets, through springs and dampers as shown in Fig. 2. The bogie model has seven degrees of freedom: lateral and yaw motion for each wheelset and the bogie frame, and roll motion of the bogie frame. In a coordinate system moving with constant speed v along the track center line, the variables are denoted $q_1, \ldots, q_7$, see Fig. 2. The speed v is chosen as the control parameter, and all other parameter values are kept constant in these investigations.

The bogie runs on a straight, horizontal, perfect track; it is assumed that the wheels and the rails remain in contact. The profile of the rail surface is an arc of a circle, and the wheels have a conical profile, with inner flange. The nonlinearities in the system stem from the creep–creep force relation at the ideal contact point between each wheel and the rail and from the flange force.

The Vermeulen–Johnson creep force law relates the resulting creep force $F_R(\xi_R)$ to the resulting creep

$$\xi_R = \sqrt{\left(\frac{\xi_x}{\Psi_1}\right)^2 + \left(\frac{\xi_y}{\Phi}\right)^2}\,,$$

where

$$\xi_{xf} = \frac{\dot{q}_1}{v} - q_2 \quad \text{and} \quad \xi_{xr} = \frac{\dot{q}_3}{v} - q_4$$

are the front and rear lateral creepages, and

$$\xi_{yf} = \frac{a\dot{q}_2}{v} + \frac{\delta q_1}{r_0} \quad \text{and} \quad \xi_{yr} = \frac{a\dot{q}_4}{v} + \frac{\delta q_3}{r_0}$$

are the front and rear longitudinal creepages. In this model $a = 0.716$ m is half the track gauge, $\delta = 0.05$ is the contact angle, and $r_0 = 0.4572$ m is the centered rolling radius of the wheel. Hertz theory is used to calculate the contact area between

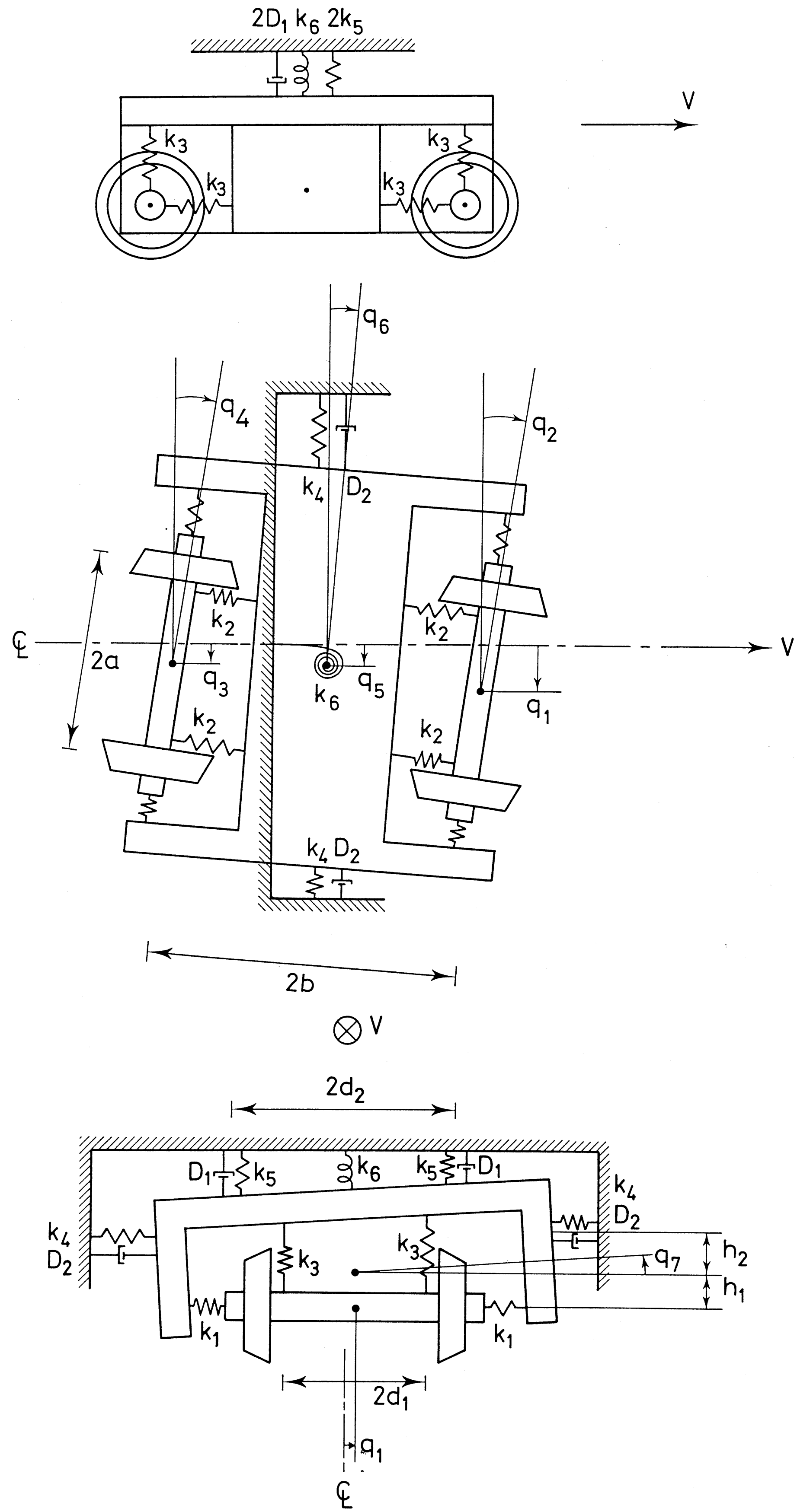

Fig. 2. Conventional bogie model.

a wheel and the rail with the coefficient of adhesion $\mu = 0.15$ and the normal force N given by $\mu N = 10$ kN. The constant G is the shear modulus and with a_e and b_e as the semiaxes of the contact ellipse, $G\pi a_e b_e = 6.563$ MN. Setting

$$u = \frac{G\pi a_e b_e}{\mu N}\xi_R$$

it follows that

$$\frac{F_R}{\mu N} = \begin{cases} u - \frac{1}{3}u|u| + \frac{1}{27}u^3 & u < 3 \\ 1 & u \geq 3 \end{cases}$$

which defines F_R. Vermeulen and Johnson [1964] show that the lateral and longitudinal creep forces are

$$F_x = \frac{\xi_x}{\Psi_1}\frac{F_R}{\xi_R} \quad \text{and} \quad F_y = \frac{\xi_y}{\Phi}\frac{F_R}{\xi_R}\,,$$

where the weight factors $\Phi = 0.60252$ and $\Psi_1 = 0.54219$ are also found in [Vermeulen & Johnson, 1964].

The flange force F_T is modeled as a stiff nonlinear spring given by

$$F_T(u) = \begin{cases} k_0(u - \eta) & \eta < u \\ 0 & -\eta \leq u \leq \eta \\ k_0(u + \eta) & -\eta > u \end{cases}$$

where we have used $k_0 = 14.60$ MN, and $\eta = 0.0091$ m.

The equations of motion for the system give seven coupled nonlinear second-order differential equations:

$$\begin{array}{llllllllll}
m_w\ddot{q}_1 & +A_1 & & & & & & & +2F_{xf} + F_T(q_1) & = 0 \\
I_{wy}\ddot{q}_2 & & & +A_3 & & & & & +2aF_{yf} + & = 0 \\
m_w\ddot{q}_3 & & +A_2 & & & & & & +2F_{xr} + F_T(q_3) & = 0 \\
I_{wy}\ddot{q}_4 & & & & +A_4 & & & & +2aF_{yr} + & = 0 \\
m_f\ddot{q}_5 & -A_1 & -A_2 & & & +A_5 & & & & = 0 \\
I_{fy}\ddot{q}_6 & -bA_1 & +A_2 & -A_3 & -A_4 & & +A_6 & & & = 0 \\
I_{fr}\ddot{q}_7 & -h_1A_1 & -h_1A_2 & & & +h_2A_5 & & +A_7 & & = 0
\end{array}$$

where

$$\begin{aligned}
A_1 &= 2k_1(q_1 - q_5 - bq_6 - h_1q_7) \\
A_2 &= 2k_1(q_3 - q_5 - bq_6 - h_1q_7) \\
A_3 &= 2k_2d_1^2(q_2 - q_6) \\
A_4 &= 2k_2d_1^2(q_4 - q_6) \\
A_5 &= 2D_2(\dot{q}_5 - h_2\dot{q}_7) + 2k_4(q_5 - h_2q_7) \\
A_6 &= k_6q_6 \\
A_7 &= 2D_1d_2^2\dot{q}_7 + 2k_5d_2^2q_7 + 4k_3d_1^2q_7
\end{aligned}$$

The front and rear, lateral and longitudinal creep forces resulting from the creepage between rails and wheels are F_{xf}, F_{yf} and F_{xr}, F_{yr}. The mass and moment of inertia of the axles are $m_w = 1022$ kg and $I_{wy} = 678$ kgm^{-2}. The mass and moment of inertia (yaw direction) of the bogie frame are $m_f = 2918$ kg and $I_{fy} = 6780$ kgm^{-2} while the moment of inertia in the roll direction is $I_{fr} = 6780$ kgm^{-2}. Other spring and damper parameters are $k_1 = 1.823$ MN/m, $k_2 = 3.646$ MN/m, $k_3 = 3.646$ MN/m, $k_4 = 0.1823$ MN/m, $k_5 = 0.3333$ MN/m, $k_6 = 2.710$ MN/m, $D_1 = 20.0$ kNs/m and $D_2 = 29.2$ kNs/m (see Fig. 2). The remaining constants $b = 1.074$ m, $h_1 = 0.0762$ m, $h_2 = 0.6584$ m, $d_1 = 0.620$ m and $d_2 = 0.680$ m are geometrical quantities (see Fig. 2).

For $n = 1, \ldots, 7$ we define

$$x_{2n-1} = q_n \quad \text{and} \quad x_{2n} = \dot{q}_n$$

and obtain an autonomous system of 14 coupled first-order differential equations with the speed v as control parameter. Abstractly, this system is:

$$\dot{x} = F(x, v)\,, \tag{1}$$

where $x \in \mathbb{R}^{14}$, $v \in \mathbb{R}^+$ and $F : \mathbb{R}^{14} \times \mathbb{R}^+ \to \mathbb{R}^{14}$.

A 14×14 matrix γ is a symmetry of this system of differential equations if

$$F(\gamma x, v) = \gamma F(x, v)$$

for all $x \in \mathbb{R}^{14}$ and $v \in \mathbb{R}^+$. The set of all symmetries of F is a group that we denote by Γ.

Let I_{14} be the 14×14 identity matrix. It is then true that $-I_{14}$ is a symmetry of F, since all the terms in F are odd in x. It follows that

$$\Gamma = \{I_{14}, -I_{14}\} \cong \mathbb{Z}_2$$

is a symmetry group for F. It is also true that Γ is the only nontrivial symmetry group of F, and F is said to be $\mathbb{Z}_2$-symmetric [Golubitsky *et al.*, 1988].

2. Theory

In this section we present the mathematical background for the numerical results discussed in the next section. In Sec. 2.1 we deduce the generic bifurcations of a system that is slightly more general than (1), and in Sec. 2.2 we discuss mode interactions in our system.

2.1. *Generic bifurcations of symmetric periodic solutions*

We consider a k-parameter family of n-dimensional systems of first-order differential equations

$$\dot{x} = F(x, \mu) \tag{2}$$

where $x \in \mathbb{R}^n$, $\mu \in \mathbb{R}^k$ and $F : \mathbb{R}^n \times \mathbb{R}^k \to \mathbb{R}^n$ has the symmetry group $\Gamma = \mathbb{Z}_2 = \{\pm I_n\}$. For convenience we set $\gamma = -I_n$.

We study the generic bifurcations of symmetric periodic solutions of (2). These ideas have been discussed previously in [Swift & Wiesenfeld, 1984; Fieldler, 1988]. Let $c(t)$ be a periodic solution of F with period T, that is,

$$c(t + T) = c(t)\,.$$

The periodic solution c is *symmetric* with respect to γ when

$$c\left(t + \frac{T}{2}\right) = \gamma c(t)\,. \tag{3}$$

Let Σ_1 be a transverse section to the periodic orbit c, and let $P : \Sigma_1 \to \Sigma_1$ be the Poincaré map. See Fig. 3. We now discuss the restrictions placed on P by the symmetry γ.

Let Σ_2 be the section given by $\Sigma_2 = \gamma\Sigma_1$, and define the mappings given by the flow: $\Theta : \Sigma_1 \to \Sigma_2$ and $\Psi : \Sigma_2 \to \Sigma_1$. See Fig. 4. Let z be a point in the section Σ_2. From the symmetry we have

$$\Psi(z) = \gamma\Theta(\gamma z)\,, \tag{4}$$

which for a given point x in the section Σ_1 yields the relation (5):

$$\begin{aligned} P(x) &= \Psi \circ \Theta(x) = \Psi(\Theta(x)) \\ &= \gamma\Theta(\gamma\Theta(x)) = (\gamma\Theta)^2(x)\,. \end{aligned} \tag{5}$$

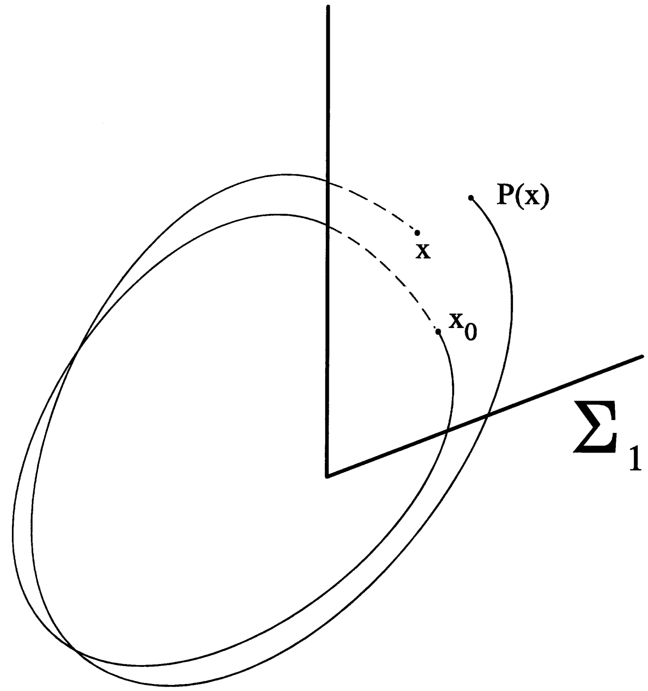

Fig. 3. Poincaré section of the flow.

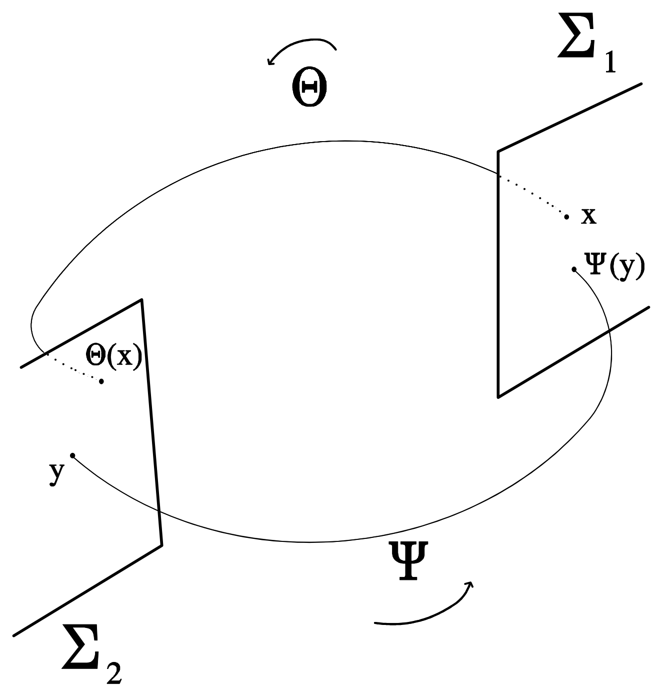

Fig. 4. Definition of the mappings, Θ and Ψ.

We define the map $Q : \Sigma_1 \to \Sigma_1$ by

$$Q = \gamma\Theta \tag{6}$$

and obtain

$$P = (\gamma\Theta)^2 = Q^2\,. \tag{7}$$

Let x_0 be the intersection of the symmetric periodic solution c with the section Σ_1 and let V be an $(n-1)$-dimensional subspace of $\mathbb{R}^n$ that is transverse to $\dot{c}(t_0)$ where $c(t_0) = x_0$. Write

$$Q : (x_0 + V) \times \mathbb{R}^k \to (x_0 + V)\,,$$

and change coordinates to obtain the map $Q : V \times \mathbb{R}^k \to V$.

By considering generic bifurcations of the map Q we deduce the generic bifurcations of the Poincaré map P and thereby the generic bifurcations from the symmetric periodic solution c.

Note that symmetric periodic solutions of F correspond to fixed points of Q. Suppose that z is the intersection of a symmetric periodic solution of F and the section Σ_1. Symmetry implies that

$$Q(z) = \gamma\Theta(z) = z\,. \tag{8}$$

Thus, a symmetric periodic solution of F corresponds to a fixed point of Q. Next let y be the intersection of an asymmetric periodic solution of F and the section Σ_1. Since the periodic solution is asymmetric we have

$$Q(y) = \gamma\Theta(y) \neq y$$

but because of the periodicity

$$Q^2(y) = P(y) = y\,. \tag{9}$$

Thus an asymmetric periodic solution of F corresponds to a period two point of the map Q.

There are three generic bifurcations of maps from fixed points: saddle-node bifurcations, Hopf bifurcations for maps (or Neimark bifurcations), and period-doubling bifurcations. These bifurcations correspond to critical eigenvalues of the linearization of the Poincaré map crossing the unit circle at $+1$, crossing as a complex conjugate pair, or crossing at -1. Generically, the bifurcations of Q and their effect on P are:

- A saddle-node bifurcation of the map Q leads to a saddle-node for the Poincaré map $P = Q^2$ and, therefore, also a saddle-node bifurcation of the periodic solution of (2).
- A Hopf bifurcation of the map Q corresponds (generically) to a Hopf bifurcation of the periodic solution of F leading to either stable or unstable quasiperiodic motion in the vicinity.
- A period-doubling bifurcation of the map Q leads to a pitchfork bifurcation of the Poincaré map $P = Q^2$ and, thereby, a pitchfork bifurcation of the flow or a symmetry breaking bifurcation.

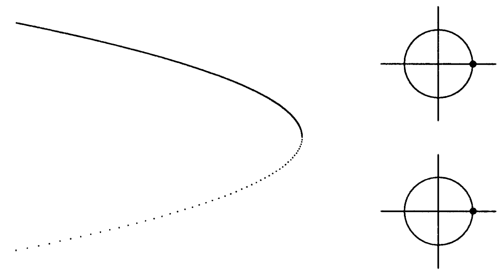

Fig. 5. Left: Saddle-node bifurcation. Upper right: Critical eigenvalue of the linearization of the Poincaré map P. Lower right: Critical eigenvalue of the linearization of the map Q.

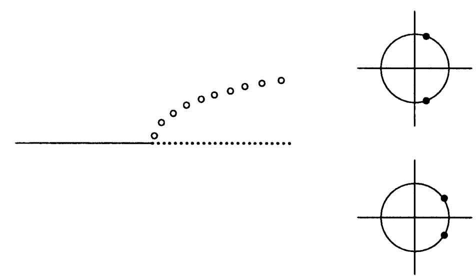

Fig. 6. Left: Hopf bifurcation. Upper right: Critical eigenvalues of the linearization of the Poincaré map P. Lower right: Critical eigenvalues of the linearization of the map Q.

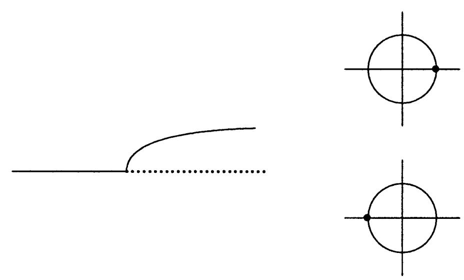

Fig. 7. Left: Pitchfork bifurcation. Upper right: Critical eigenvalue of the linearization of the Poincaré map P. Lower right: Critical eigenvalue of the linearization of the map Q.

Note that period-doubling bifurcations of symmetric periodic solutions are *not* generic.

The generic bifurcations of symmetric periodic solutions of (2) are listed in Figs. 5–7. Note that the two bifurcating asymmetric periodic solutions in Fig. 7 coincide in our choice of illustration.

2.2. *Mode interaction*

The eigenspaces associated with the Jacobian matrix are often called *modes*. Generically, in one-parameter systems, we expect to have only one critical mode at a time (a critical mode corresponds to a critical eigenvalue). By varying another parameter, multiple critical modes are possible. Near parameter values at which there are multiple critical modes different types of secondary bifurcations may occur. These secondary solutions are created by nonlinear interactions of the two modes and are called *mode interactions*.

Suppose that a saddle-node point and a period-doubling point for the map Q occur simultaneously at the origin (by varying two parameters at a time). Define the mapping $R : V \times V \times \mathbb{R}^k \to V \times V$ given by

$$R(\sigma, \rho, \mu) = (Q(\sigma, \mu) - \rho, Q(\rho, \mu) - \sigma) \tag{10}$$

for all $\sigma, \rho \in V$ and $\mu \in \mathbb{R}^k$.

Note that zeroes of R correspond to either fixed points or period two points of Q. Thus, it is possible to study the bifurcations of fixed points and period two points of Q by studying the bifurcation of zeroes of R, and the bifurcation of zeroes has been well studied, see e.g. [Golubitsky & Schaeffer, 1985].

To look for bifurcation of zeroes of R, we need to find zero eigenvalues of the linearization L of the map R evaluated at the origin. The map L is

$$L = dR|_0 = \begin{pmatrix} \dfrac{\partial Q}{\partial \sigma}(0) & -I \\ -I & \dfrac{\partial Q}{\partial \rho}(0) \end{pmatrix}. \tag{11}$$

Assume that v is an eigenvector of the linearization of Q corresponding to the critical eigenvalue $+1$ (the saddle-node) and that w is an eigenvector of the linearization of Q corresponding to the critical eigenvalue -1 (the period-doubling). We find

$$L\begin{pmatrix} v \\ v \end{pmatrix} = \begin{pmatrix} \dfrac{\partial Q}{\partial \sigma}(0) & -I \\ -I & \dfrac{\partial Q}{\partial \rho}(0) \end{pmatrix} \begin{pmatrix} v \\ v \end{pmatrix} = \begin{pmatrix} v - v \\ -v + v \end{pmatrix} = \underline{0},$$

and

$$L\begin{pmatrix} w \\ -w \end{pmatrix} = \begin{pmatrix} \dfrac{\partial Q}{\partial \sigma}(0) & -I \\ -I & \dfrac{\partial Q}{\partial \rho}(0) \end{pmatrix} \begin{pmatrix} w \\ -w \end{pmatrix} = \begin{pmatrix} -w - (-w) \\ -w - (-w) \end{pmatrix} = \underline{0}.$$

Thus

$$\ker L = \operatorname{span}\left(\begin{pmatrix} v \\ v \end{pmatrix}, \begin{pmatrix} w \\ -w \end{pmatrix}\right) \tag{12}$$

and a Lyapunov–Schmidt reduction leads to a dynamical system in a two-dimensional space that is tangential to ker L at the origin [Golubitsky & Schaeffer, 1985, Chap. VII]. Now we determine the characteristics of such a system.

Let κ act on V^2 by

$$\kappa(\sigma, \rho) = (\rho, \sigma)$$

for all $\sigma, \rho \in V$. Note that κ is a symmetry of R since

$$\begin{aligned} \kappa R(\sigma, \rho, \mu) &= \kappa(Q(\sigma, \mu) - \rho, Q(\rho, \mu) - \sigma) \\ &= (Q(\rho, \mu) - \sigma, Q(\sigma, \mu) - \rho) \\ &= R(\rho, \sigma, \mu) \\ &= R\kappa(\sigma, \rho, \mu). \end{aligned}$$

Observe that κ acts on (v, v) and $(w, -w)$ by

$$\kappa(v, v) = (v, v)$$
$$\kappa(w, -w) = (-w, w) = -(w, -w).$$

Thus we can determine the action of κ on ker L. We write the vectors in ker L as

$$x(v, v) + y(w, -w);$$

we can then identify ker $L \cong \mathbb{R}^2$ using the coordinates $(x, y) \in \mathbb{R}^2$. Since

$$\kappa(x(v, v) + y(w, -w)) = x(v, v) - y(w, -w),$$

the action of κ on $\mathbb{R}^2 \cong$ ker L is given by

$$\kappa(x, y) = (x, -y).$$

Since the Lyapunov–Schmidt reduction respects symmetry, we find that the zeroes of R are parametrized by the zeroes of a map $T : \mathbb{R}^2 \times \mathbb{R}^k \to \mathbb{R}^2$ that satisfies

$$T(\kappa(x, y), \mu) = \kappa T(x, y, \mu).$$

Thus we have a system in two state variables with $\mathbb{Z}_2$-symmetry, $(x, y) \to (x, -y)$. The bifurcations in this case have been studied by Dangelmayr and Armbruster [1983] and they are described in [Golubitsky *et al.*, 1988, Chap. XIX, §§2–3]. In the next section, we present an example of such a mode interaction that is also found in our bogie model.

3. Results

In this section we discuss those results from our numerical investigations of the mathematical model of the railway bogie presented in Sec. 1 that can be analyzed by the mathematical tools presented in Sec. 2. Other interesting features of the mathematical model have been presented elsewhere [Jensen & True, 1997; True, 1993].

The main numerical tool for the analysis of this model is the continuation routine PATH [Kaas-Petersen, 1989] developed by Kaas-Petersen. It is our experience that numerical tools such as PATH are most efficient away from critical parameter values. Near the critical parameter values one often must inspect carefully whether the numerical tool does what you ask and expect it to do, with respect to the mathematical theory.

We first fix all parameters but the control parameter (the speed) v and we study the solutions of the dynamical system. It is easily seen that the fixed point $x_1 = \cdots = x_{14} = 0$ is an equilibrium solution for all values of v. For low speeds the solution is asymptotically stable, but at $v = 65.2$ m/s the solution loses stability in a Hopf bifurcation. The bifurcating periodic solution is symmetric with respect to the symmetry group presented in Sec. 1 and bifurcates subcritically and it is unstable. At $v = 63.64$ m/s the solution turns around and stabilizes in a saddle-node bifurcation. We have managed to follow the symmetric periodic solution as it undergoes five saddle-node bifurcations, three pitchfork bifurcations and one Hopf bifurcation. The details are summarized in Table 1. The data from Table 1 are depicted in Figs. 8 and 9. Note that stable periodic solutions are depicted by solid lines and unstable periodic solutions are depicted by dotted lines.

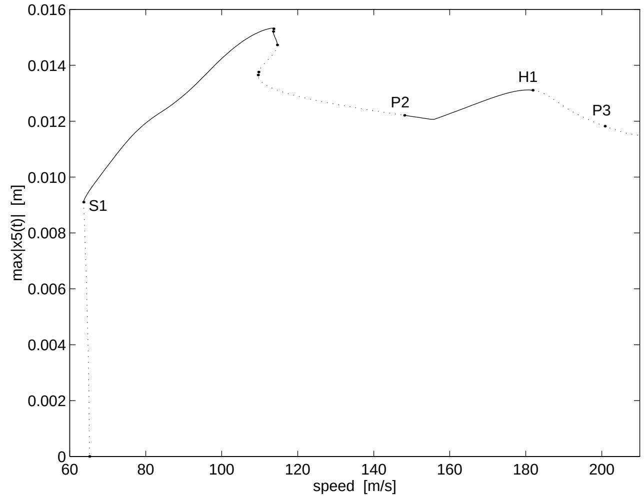

Fig. 8. The symmetric periodic solutions with its bifurcations.

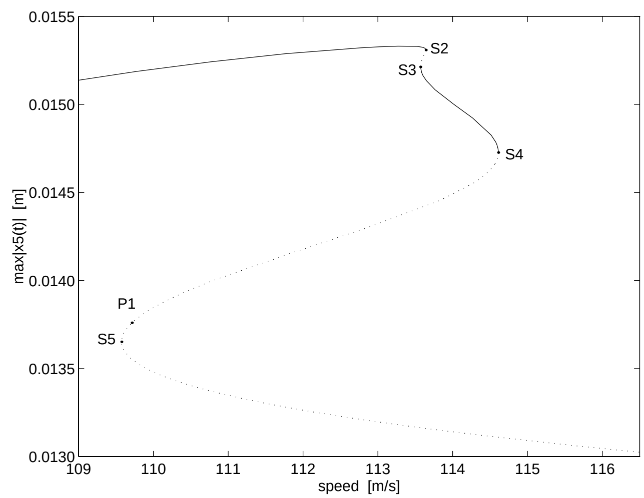

Fig. 9. Blow up of Fig. 8.

Table 1. Bifurcations along symmetric periodic solution bifurcating from stationary solution at A.

Name	Speed	Bifurcation Type
A	65.20 m/s	Hopf
S_1	63.64 m/s	Saddle-node
S_2	113.64 m/s	Saddle-node
S_3	113.57 m/s	Saddle-node
S_4	114.61 m/s	Saddle-node
P_1	109.70 m/s	Pitchfork
S_5	109.58 m/s	Saddle-node
P_2	147.59 m/s	Pitchfork
H_1	181.73 m/s	Hopf
P_3	200.87 m/s	Pitchfork

The final bifurcation diagram is shown in Fig. 10. Figures 11 and 12 show the details in the complex region 109 m/s $< v <$ 115 m/s. It is noticeable that in the region 115 m/s $< v <$ 147 m/s the only stable periodic solutions are the asymmetric ones bifurcating from the symmetric periodic solution at P_1. The asymmetric periodic solutions bifurcate subcritically, turn around in a saddle-node, gain stability in a Hopf bifurcation (Neimark bifurcation) at $v = 112.59$ m/s and remain stable up to $v = 203.33$ m/s where they lose stability in another Hopf bifurcation (Neimark bifurcation). The symmetric periodic solution is stable

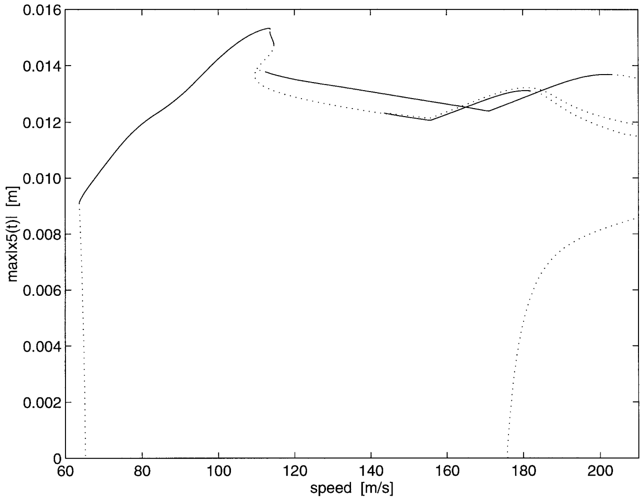

Fig. 10. Final bifurcation diagram.

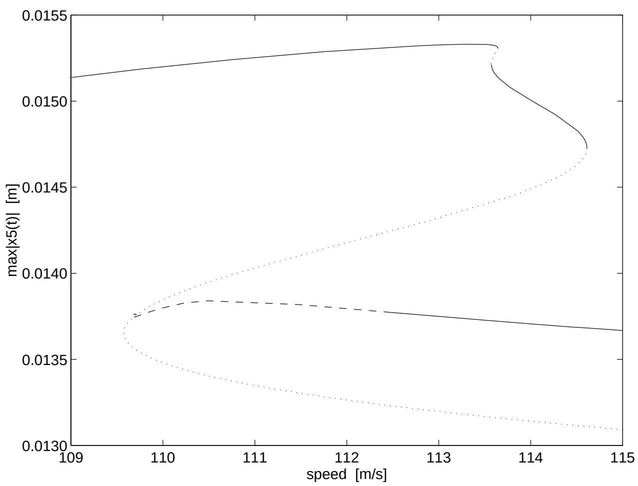

Fig.11. Blow up of Fig. 10.

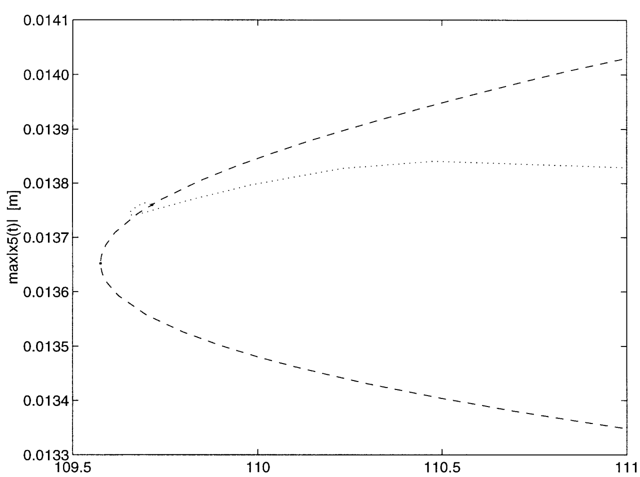

Fig. 12. Blow up of Fig. 10. NB! $b = 1.074$ m.

in the region 147.59 m/s $< v <$ 181.73 m/s but, as found by Galvanetto *et al.* [1997], the symmetric periodic solution in this region is a "secondary" solution with a much smaller basin of attraction than the asymmetric periodic solutions. Thus, in the region 115 m/s $< v < 200$ m/s, the asymmetric periodic solutions are *dominant*.

In Fig. 12 we see the details of the final bifurcation diagram in the speed interval 109.5 m/s $<$ $v < 110$ m/s showing an example of mode interaction. The figure shows the region near the pitchfork bifurcation P_1 and the saddle-node bifurcation S_5. The dashed curve in Fig. 12 is the symmetric periodic solution and the dotted curve is the bifurcating asymmetric periodic solution. The saddle-node point and the pitchfork point are very close in parameter space. This is exactly the situation we considered in Sec. 2.2. There we found that the case could be described locally by a system with two state space variables possessing the symmetry $(x, y) \to (x, -y)$. Referring to [Golubitsky *et al.*, 1988, p. 425], we find that Fig. XIX.3.5 in [Golubitsky *et al.*, 1988, p. 431] is identical to our Fig. 12. The asterisk along the asymmetric solution in [Golubitsky *et al.*, 1988, Fig. XIX.3.5, p. 431] indicates that a Hopf bifurcation of this solution is possible. In fact, that is exactly what we find in the bogie model; the asymmetric periodic solutions gain stability in a Hopf bifurcation (Neimark bifurcation) at $v = 112.59$ m/s. Thus, referring to [Golubitsky *et al.*, 1988, p. 425], we can conclude that in the vicinity of the mode interaction, the dynamics of our system can locally be described by the two state variable systems with the normal form

$$(x^2 + y^4 - \beta y^2 - \lambda,\ -(x - \alpha)y) \qquad (13)$$

with $\alpha > 0$ and $\beta \in]0, 2\alpha[$.

Changing now the parameter b to $b = 1.085$ m we obtain the bifurcation diagram in the vicinity of the mode interaction found in Fig. 13. Referring to [Golubitsky *et al.*, 1988, p. 425] again, we see that now the dynamics of the system can locally be described by the (same) two state variable systems with the normal form (13) and with $\alpha > 0$ and $\beta < 0$.

Changing the parameter b further to $b =$ 1.100 m we obtain the bifurcation diagram in the vicinity of the mode interaction found in Fig. 14. With this value of the parameter b, the dynamics of the bogie system can locally be described by the normal form (13) with $\alpha < 0$ and $\beta < 0$.

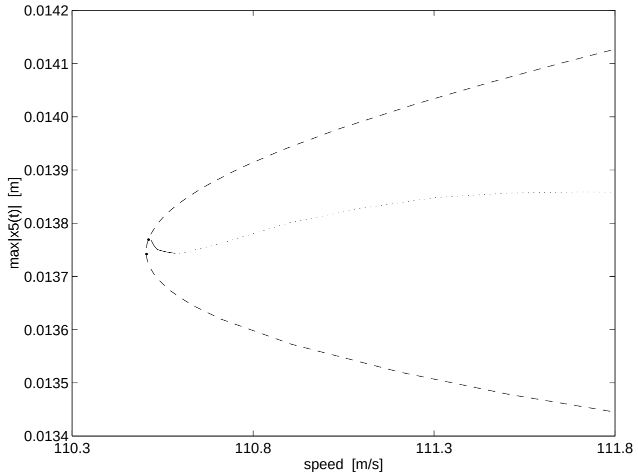

Fig. 13. Bifurcation diagram near mode interaction with $b = 1.085$ m.

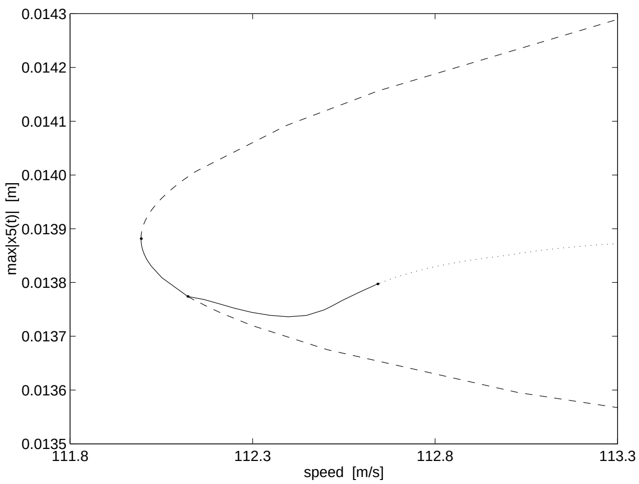

Fig. 14. Bifurcation diagram near mode interaction with $b = 1.100$ m.

It should be noted that in Figs. 12–14 we have depicted the unstable parts of the symmetric periodic solutions by dashed lines, and the unstable parts of the asymmetric periodic solutions by dotted lines.

From a mathematical point of view it has been quite pleasing to find numerically the local bifurcation scenarios in Figs. 12–14, which are practically identical to the bifurcation diagrams predicted by unfolding the corresponding codimension 2 bifurcation in [Golubitsky *et al.*, 1988, p. 425].

4. Conclusion

We have considered the Cooperrider model of a railway bogie. This model has been investigated by several authors. The present work analyzes the bifurcations using symmetry groups. We find that the model is $\mathbb{Z}_2$-symmetric, so the equations of motion can be written in the form

$$\dot{x} = F(x, v)$$

where $x \in \mathbb{R}^{14}$ and $v \in \mathbb{R}^{+}$. This differential equation has the symmetry property

$$F(\gamma x, v) = \gamma F(x, v)$$

for $\gamma = -I_{14}$.

We then develop the generic bifurcations of symmetric periodic solutions of a system on that form, considering the Poincaré map P and a map Q with the property $P = Q^2$. The numerical bifurcation analysis of our system has revealed many bifurcations in the system, all of them generic in the sense described in Sec. 2.

Section 2.2 deals with the theory for the dynamics of the system near the parameter values where bifurcation points of low codimension coincide. We consider the form of the mode interaction in such a situation. The numerical bifurcation analysis of our system reveals a very complicated region where a mode interaction as described in Sec. 2.2 and [Golubitsky *et al.*, 1988, Chap. XIX, §§2–3] takes place. This mode interaction yields the information necessary to complete the bifurcation diagram of our bogie model. The splitting and the correct sequence of the bifurcations in the complicated region was found after studies of the stringent mathematical theory for symmetry and bifurcations. The theory verified the numerical results and helped the authors to refine the numerical investigations until only generic bifurcations appeared in the bogie model. Furthermore, these refined investigations revealed the continuation of the symmetric periodic solution. This solution is unstable for a large speed range but gains stability in the speed range 147.59 m/s $< v <$ 181.73 m/s. In this speed range, however, the asymmetric periodic solution is dominant, and the symmetric periodic solution had not been found in earlier investigations, due to its small basin of attraction.

From the mode interaction in the complicated region, the theory in [Golubitsky *et al.*, 1988, Chap. XIX, §§2–3] also predicts the Neimark bifurcation in the bogie system and the presence of a quasiperiodic solution bifurcating from the asymmetric periodic solution. This quasiperiodic attractor, its development and its symmetry characteristics have been studied in [Jensen & True, 1997].

Asymmetric wear of railway wheelsets do occur in real life. We suggest that this lopsided wear under certain conditions may be related to a symmetry breaking pitchfork bifurcation as described in this paper.

The Cooperrider bogie is a realistic model of a passenger car bogie, but the model of the wheel/rail contact is highly simplified. Today real wheel profiles have varying curvature. They are not plainly conical, but as long as the amplitudes of the lateral oscillations are sufficiently small the curved profile may be approximated by a conical one. The most unrealistic assumption in the model is that a linear spring with a dead band can model the flange contact. The sudden action of the spring has the character of an elastic impact which in all probability is alone responsible for the complicated dynamics in the speed range that is investigated in this article. Such events are however interesting also in vehicle systems dynamics, because the dynamical effects of simple motion delimiters, which are often used in the constructions, are unknown.

Passenger cars are usually not run at speeds higher than the nonlinear critical speed. It may however happen that the critical speed has decreased below the operating speed due to heavily worn wheel profiles, and it is therefore important to know what can happen at speeds higher than the critical speed. The fastest trains today have a service speed of 300 km/h $\sim$ 83.3 m/s, but trains with service speeds up to 350–360 km/h $\sim\leq$ 100 m/s are under development. Due to aerodynamic effects and economy a service speed of 350 km/h is deemed the highest economically and technically feasible speed of passenger trains today.

Freight car bogies are similar to passenger bogies in design but simpler — and cheaper — in construction. Freight cars are frequently moved at speeds greater than their nonlinear critical speed, which is influenced by motion delimiters and dry friction dampers. These elements constitute the main difficulties in an accurate modeling of the dynamics of freight cars, but we can still gain valuable information about what to expect from dynamically simpler bogie designs like the Cooperrider bogie.

Acknowledgments

This work was supported by Otto Mønsted's Foundation Grant 93-33-1233 and The Danish Council for Scientific and Industrial Research Grant n. 16-4786.M. The research of MG was supported in part by NSF Grant DMS-9403624. The Department of Mathematics of the University of Houston is kindly acknowledged for hosting Carsten Nordstrøm Jensen during a part of this work and for the use of its computing facilities.

References

Cooperrider, N. K. [1972] "The hunting behaviour of conventional railway trucks," *J. Engin. Industry* **94**, 752–762.

Dangelmayr, G. & Armbruster, D. [1983] "Classification of $\mathbb{Z}_2$-equivariant imperfect bifurcations of corank 2," *Proc. London Math. Soc.* **46**, 517–546.

Fiedler, B. [1988] *Global Bifurcations of Periodic Solutions with Symmetry*, Lecture Notes in Mathematics **1309** (Springer-Verlag, Berlin).

Galvanetto, U., Briseghella, L. & Bishop, S. R. [1997] "Optimal axle distance of a railway bogie," *Int. J. Bifurcation and Chaos* **7**(3), 721–732.

Golubitsky, M. & Schaeffer, D. G. [1985] *Singularities and Groups in Bifurcation Theory*, Vol. 1 (Springer-Verlag).

Golubitsky, M., Stewart, I. & Schaeffer, D. G. [1988] *Singularities and Groups in Bifurcation Theory*, Vol. 2 (Springer-Verlag).

Jensen, C. N. [1994] "Symmetry in nonlinear railway dynamics," Master's Thesis, Department of Mathematical Modelling, The Technical University of Denmark.

Jensen, C. N. & True, H. [1997] "On a new route to chaos in railway dynamics," *Nonlin. Dyn.* **13**, 117–129.

Kaas-Petersen, C. [1989] *PATH — User's Guide*, Department Applied Mathematics Studies & Centre Nonlinear Studies, University Leeds.

Swift, J. W. & Wiesenfeld, K. [1984] "Suppression of period doubling in symmetric systems," *Phys. Rev. Lett.* **52**(9), 705–708.

True, H. [1993] "Some recent developments in nonlinear railway vehicle dynamics," in *1st European Nonlinear Oscillations Conf.*, eds. Kreuzer, E. & Schmidt, G., *Proc. Int. Conf. Hamburg*, Berlin, August (Akademie Verlag), pp. 129–148.

Vermeulen, P. J. & Johnson, K. L. [1964] "Contact of nonspherical elastic bodies transmitting tangential forces," *J. Appl. Mech.* **31**, 338–340.